Search for a doubly-charged boson in four-lepton final states in type II seesaw

CrossMark

Eung Jin Chun, Pankaj Sharma *

Korea Institute for Advanced Study, Seoul 130-722, Republic of Korea

A B S T R A C T

CMS and ATLAS have searched for a doubly-charged boson $H^{\pm\pm}$ which may arise from type II seesaw in the 7 TeV run at the LHC by considering pair or associated production of doubly-charged bosons under the assumption of degenerate triplet scalars. In this work, we consider non-degenerate triplet components with the mass gap $\Delta M \sim 1$–40 GeV which leads to enhanced pair-production cross-sections of $H^{\pm\pm}$ added by the gauge decays of the heavier neutral and singly-charged bosons. We reevaluate the constraints in the ΔM–$M_{H^{++}}$ plane depending on the triplet vacuum expectation value v_Δ in the type II seesaw model which are much more stringent than the current search limits. We further study the possibility of observing same-sign tetra-lepton signals in the allowed parameter space which can be probed in the future runs of the LHC.

© 2013 The Authors. Published by Elsevier B.V. Open access under CC BY license.

1. Introduction

One of the key questions in physics beyond Standard Model is the origin of the neutrino masses and mixing. It can be attributed to an $SU(2)$ triplet boson which couples to both the lepton doublet fermions and the Higgs doublet boson realizing the so-called type II seesaw mechanism [1]. An essential feature of this scenario is the presence of a doubly-charged boson $H^{\pm\pm}$ whose decay to same-sign di-leptons with different flavor states may allow us to probe the neutrino mass structure at the LHC [2]. CMS [3] and AT-LAS [4] have searched for doubly-charged bosons at $\sqrt{s} = 7$ TeV with about 5 fb^{-1} of integrated luminosity of data. CMS have considered three- and four-lepton final states coming from the associated production process $pp \to H^{++}H^- \to \ell_i^+\ell_j^+\ell_k^-\nu_l$ [5–7] and the pair-production process $pp \to H^{++}H^{--} \to \ell_i^+\ell_j^+\ell_k^-\ell_l^-$ [8] to put constraints on the doubly-charged boson mass $M_{H^{++}}$ in four different benchmark points that would probe different neutrino mass structure. On the other hand, ATLAS looked at same-sign di-lepton (SS2L) signals to probe $H^{\pm\pm}$ in pair-production of doubly-charged boson at the LHC. In their analysis, they put strong bound on leptonic branching fractions of the doubly-charged boson depending on its mass.

In both analyses, degenerate masses for the triplet bosons, $H^{\pm\pm}$, $H^\pm$, H^0 and A^0 are assumed, which is possible only when

a particular scalar coupling called λ_5 in the scalar potential vanishes. But there is no reason to assume this particular coupling to be zero. Indeed, interesting phenomena arise for non-vanishing λ_5 [2,9–11]. When λ_5 is positive leading to $\Delta M \equiv M_{H^+} - M_{H^{++}} \approx M_{H,A} - M_{H^+} > 0$, $H^{\pm\pm}$ is the lightest among triplet scalars and other triplet scalars decay dominantly to $H^{\pm\pm}$ through cascade decay associated with several $W^{\mp*}$ in a large parameter space of λ_5.[1] In this parameter space, pair-production cross-section is enhanced significantly since other (pair and associated) triplet production channels contribute to pair-production of doubly-charged bosons through the cascade decays of the pair/associate-produced heavier components $H^\pm$ or H^0/A^0: $H^0/A^0 \to H^\pm W^\mp \to H^{\pm\pm}W^\mp W^\mp$. This leads to a more stringent bound on doubly-charged boson mass $M_{H^{++}}$ as compared to the current CMS and ATLAS bounds.

In this Letter, we evaluate the exclusion regions in the $M_{H^{++}}$–ΔM plane in the type II seesaw model utilizing the search strategy employed by CMS and ATLAS Collaborations. We consider λ_5 (and thus ΔM) to be non-vanishing and thus expect much stronger bound on $M_{H^{++}}$ than obtained by CMS and ATLAS. This bound depends also on the triplet vacuum expectation value v_Δ which controls the ratio of the branching fractions for $H^{++} \to l_i^+ l_j^+$ and $W^+ W^+$ through the neutrino mass relation [2]. For the illustration of our analysis, we choose three different values of v_Δ to examine the parameter regions of $(M_{H^{++}}, \Delta M)$ allowed by the current data and then look for the possibility of observing same-sign tetra-lepton (SS4L) signal [13] at 8 TeV LHC (LHC8), and

---

[1] The mass gap ΔM is restricted by $|\Delta M| \lesssim 40$ GeV independently of $M_{H^{++}}$ due to electroweak precision constraints [12] and thus the associated $W^\pm$ are always off-shell.

* Corresponding author.

13 TeV LHC (LHC13) with 20 fb^{-1} and 100 fb^{-1} integrated luminosities, respectively. When $v_\Delta \gg 10^{-4}$ GeV, the branching fraction of $H^{++} \to W^+ W^+$ is almost 100% resulting in highly suppressed same-sign di-lepton [14] or four-lepton signals [15] from W decays and thus very loose bounds on $M_{H^{++}}$. We take v_Δ as large as 2×10^{-4} GeV for which the branching fraction of $H^{++} \to l^+ l^+$ is around 20% and thus still a sizable number of four-lepton final states can arise. Note that SS4L signals arise due to a novel phenomenon of the triplet–antitriplet oscillation guaranteed by a tiny mass splitting between H^0 and A^0 related to the neutrino mass, which leads to pair-production of same-sign doubly-charged bosons after the chain decays of $H^0, A^0 \to H^\pm \to H^{\pm\pm}$ allowed by sizable ΔM [13].

2. Type II seesaw model

When the Higgs sector of the Standard Model is extended to have a $Y = 1$ complex $SU(2)_L$ scalar triplet Δ in addition to the standard doublet Φ, the gauge-invariant Lagrangian is written as

$$\mathcal{L} = (D_\mu \Phi)^\dagger (D^\mu \Phi) + \text{Tr}(D_\mu \Delta)^\dagger (D^\mu \Delta) - \mathcal{L}_Y - V(\Phi, \Delta)$$

where the leptonic part of the Lagrangian required to generate neutrino masses is

$$\mathcal{L}_Y = f_{ij} L_i^T C i\tau_2 \Delta L_j + \text{H.c.} \tag{1}$$

and the scalar potential is

$$\begin{aligned}
V(\Phi, \Delta) &= m^2 \Phi^\dagger \Phi + \lambda_1 (\Phi^\dagger \Phi)^2 + M^2 \text{Tr}(\Delta^\dagger \Delta) + \lambda_2 [\text{Tr}(\Delta^\dagger \Delta)]^2 \\
&\quad + \lambda_3 \text{Det}(\Delta^\dagger \Delta) + \lambda_4 (\Phi^\dagger \Phi) \text{Tr}(\Delta^\dagger \Delta) \\
&\quad + \lambda_5 (\Phi^\dagger \tau_i \Phi) \text{Tr}(\Delta^\dagger \tau_i \Delta) \\
&\quad + \left[\frac{1}{\sqrt{2}} \mu (\Phi^T i\tau_2 \Delta \Phi) + \text{H.c.} \right].
\end{aligned} \tag{2}$$

Here used is the 2×2 matrix representation of Δ:

$$\Delta = \begin{pmatrix} \Delta^+/\sqrt{2} & \Delta^{++} \\ \Delta^0 & -\Delta^+/\sqrt{2} \end{pmatrix}. \tag{3}$$

Upon the electroweak symmetry breaking with $\langle \Phi^0 \rangle = v_0/\sqrt{2}$, the μ term in Eq. (2) gives rise to the vacuum expectation value of the triplet $\langle \Delta^0 \rangle = v_\Delta/\sqrt{2}$ where $v_\Delta \approx \mu v_0^2/\sqrt{2} M^2$. For non-vanishing v_Δ, the neutrino mass matrix is generated as a product of the leptonic Yukawa coupling (1) and v_Δ:

$$M_{ij}^\nu = f_{ij} v_\Delta. \tag{4}$$

This allows us to reconstruct the Yukawa matrix f_{ij} from the current neutrino oscillation data up to unmeasured CP phases and mass hierarchy. For our analysis, we use two neutrino mass matrices for normal and inverted hierarchies derived in Ref. [13] assuming vanishing CP phases.

After the electroweak symmetry breaking, there are seven physical massive scalar eigenstates denoted by $H^{\pm,\pm}$, $H^\pm$, H^0, A^0, h^0. Under the condition that $|\xi| \ll 1$ where $\xi \equiv v_\Delta/v_0$, the first five states are mainly from the triplet scalar and the last from the doublet scalar. For the neutral pseudoscalar and charged scalar parts,

$$\begin{aligned}
\phi_I^0 &= G^0 - 2\xi A^0, & \phi^+ &= G^+ + \sqrt{2}\xi H^+, \\
\Delta_I^0 &= A^0 + 2\xi G^0, & \Delta^+ &= H^+ - \sqrt{2}\xi G^+
\end{aligned} \tag{5}$$

where G^0 and G^+ are the Goldstone modes, and for the neutral scalar part,

$$\begin{aligned}
\phi_R^0 &= h^0 - a\xi H^0, \\
\Delta_R^0 &= H^0 + a\xi h^0
\end{aligned} \tag{6}$$

where $a = 2 + 4(4\lambda_1 - \lambda_4 - \lambda_5) M_W^2/g^2 (M_{H^0}^2 - M_{h^0}^2)$. Neglecting the triplet–doublet mixing, the masses of the triplet bosons are

$$M_{H^{\pm\pm}}^2 = M^2 + 2\frac{\lambda_4 - \lambda_5}{g^2} M_W^2,$$

$$M_{H^\pm}^2 = M_{H^{\pm\pm}}^2 + 2\frac{\lambda_5}{g^2} M_W^2,$$

$$M_{H^0, A^0}^2 = M_{H^\pm}^2 + 2\frac{\lambda_5}{g^2} M_W^2. \tag{7}$$

The mass of the Standard Model boson h^0 is given by $m_{h^0}^2 = 4\lambda_1 v_\Phi^2$ as usual.

Eq. (7) tells us that the mass splitting among triplet scalars to the linear order for small splitting (that is, for $|\lambda_5| M_W \ll gM$) can be written as

$$\Delta M \approx \frac{\lambda_5 M_W}{g}. \tag{8}$$

Furthermore, depending upon the sign of the coupling λ_5, there are two mass hierarchies among the triplet components: $M_{H^{\pm\pm}} > M_{H^\pm} > M_{H^0/A^0}$ for $\lambda_5 < 0$; or $M_{H^{\pm\pm}} < M_{H^\pm} < M_{H^0/A^0}$ for $\lambda_5 > 0$. In this work, we focus on the latter scenario, where the doubly-charged scalar $H^{\pm\pm}$ is the lightest so that it decays only to $l_i^\pm l_j^\pm$ or $W^\pm W^\pm$ whose coupling constants are proportional to f_{ij} or ξ, respectively:

$$\mathcal{L} = \frac{1}{\sqrt{2}} \left[f_{ij} \bar{l}_i^c P_L l_j + g\xi M_W W^- W^- \right] H^{++} + \text{h.c.} \tag{9}$$

Thus the branching fraction for $H^{++} \to l_i^+ l_j^+$ is completely determined for given v_Δ and the neutrino matrix (4). On the other hand, H^0/A^0 ($H^\pm$) decays mainly to $H^\pm W^{\mp*}$ ($H^{\pm\pm} W^{\mp*}$) unless the mass splitting ΔM is negligibly small.

The di-lepton decay rates of H^{++} are given by

$$\Gamma_{l_i l_j} \equiv \Gamma(\Delta^{++} \to l_i^+ l_j^+) = S \frac{|f_{ij}|^2}{16\pi} M_{\Delta^{++}} \tag{10}$$

where $S = 2$ (1) for $i \neq j$ ($i = j$). From the neutrino mass relation, $M_{ij}^\nu = f_{ij} v_\Delta$, one gets the total di-lepton rate which is inversely proportional to v_Δ^2:

$$\Gamma_{ll} \equiv \sum_{i,j} \Gamma_{l_i l_j} = \frac{1}{16\pi} \frac{\bar{m}_\nu^2}{v_\Delta^2} M_{\Delta^{++}} \tag{11}$$

where $\bar{m}_\nu^2 = \sum_i m_{\nu_i}^2$ is the sum of three neutrino mass-squared eigenvalues. On the other hand, the di-W decay rate $\Gamma_{WW} = \Gamma(H^{++} \to W^+ W^+)$ is proportional to v_Δ^2, and thus the leptonic branching fraction $\text{BF}(H^{++} \to l^+ l^+) \equiv \Gamma_{ll}/\Gamma_{H^{++}}$ is a sensitive function of v_Δ. In Fig. 1, we provide a plot for the leptonic branching fraction depending on v_Δ for two values of $M_{H^{++}} = 200$ and 500 GeV, reproducing the previous results [6,11,14] though for different H^{++} masses. For our collider analysis in the following sections, we will take three example values of v_Δ to discuss the dependence on the leptonic branching fraction and the mass gap.

Given the neutrino mass matrices for the normal (NH) and inverted (IH) hierarchies [13], the individual di-lepton decay rates $\Gamma_{l_i l_j}$ normalized by the total leptonic decay rate Γ_{ll} are given by

$\Gamma_{l_i l_j}/\Gamma_{ll}$ (%)	ee	$e\mu$	$e\tau$	$\mu\mu$	$\mu\tau$	$\tau\tau$	
NH	0.62	5.11	0.51	26.8	35.6	31.4	(12)
IH	47.1	1.27	1.35	11.7	23.7	14.9	
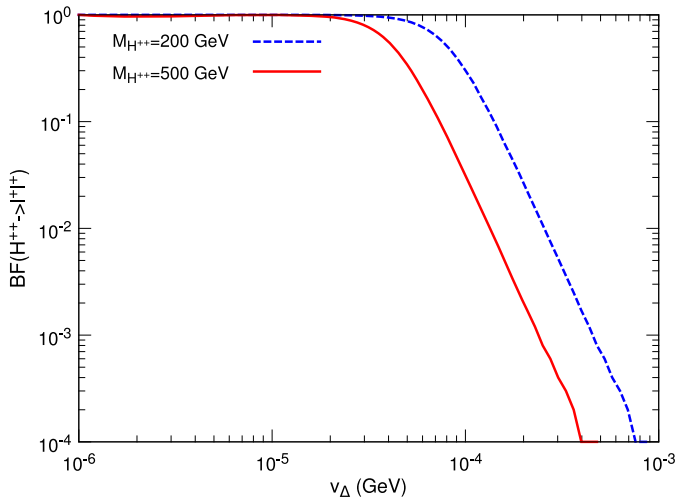
Fig. 1. Branching fraction of $H^{++} \to \ell^+\ell^+$ as a function of triplet vacuum expectation value v_Δ for $M_{H^{++}} = 200$ GeV and 500 GeV.

For given v_Δ one can read off the flavor-dependent branching fraction BF($H^{++} \to l_i^+ l_j^+$) $= \Gamma_{l_i l_j}/\Gamma_{H^{++}}$ combining Eq. (12) and Fig. 1.

An important quantity for an SS4L signal is the mass splitting δM_{HA} between H^0 and A^0 which is much smaller than the mass difference ΔM between different triplet components. The μ term in Eq. (2), which is lepton number violating, generates not only the triplet VEV:

$$v_\Delta = \frac{\mu v_0^2}{\sqrt{2} M_{H^0}^2},$$ (13)

but also the mass splitting between the heavy neutral scalars, $\delta M_{HA} \equiv M_{H^0} - M_{A^0}$:

$$\delta M_{HA} = 2 M_{H^0} \frac{v_\Delta^2}{v_0^2} \frac{M_{H^0}^2}{M_{H^0}^2 - m_{h^0}^2}.$$ (14)

As will be shown later, δM_{HA} can be comparable to the total decay rate of the neutral scalars, Γ_{H^0/A^0}, for a preferable choice of v_Δ, which enhances the same-sign tetra-lepton signal [13].

3. Constraining $\Delta M - M_{H^{\pm\pm}}$ from SS2L signals

As stated earlier, CMS and ATLAS both have assumed degenerate triplet scalars and thus could only study the process $pp \to H^{++}H^{--}$ in their analyses. In type II seesaw model, when scalar coupling $\lambda_5 > 0$, there are several triplet scalar production processes which can contribute to pair-production of doubly-charged bosons which are listed below:

1. $pp \to H^{\pm\pm}H^{\mp}$ followed by $H^{\mp} \to H^{\mp\mp}W^{\pm*}$,
2. $pp \to H^{\pm}H^{\mp}$ followed by $H^{\mp} \to H^{\mp\mp}W^{\pm*}$,
3. $pp \to H^{\pm}H^0/A^0$ followed by $H^0/A^0 \to H^{\mp}W^{\pm*}$ and $H^{\pm} \to H^{\pm\pm}W^{\mp*}$.

In Fig. 2, we plot the branching fraction of $H^{\pm} \to H^{\pm\pm}W^{\mp*}$ in the $v_\Delta - \Delta M$ plane. Similar analysis has been made in Refs. [9–11, 13]. The purple and pink regions denote the parameter space where BF($H^{\pm} \to H^{\pm\pm}W^{\mp*}$) is greater than 90% and 50% respectively. As can be seen from the figure that when there is non-zero mass splitting among the triplet scalars, there can be large parameter space where this BF is dominant. Furthermore this would lead to a significant enhancement in the number of events for
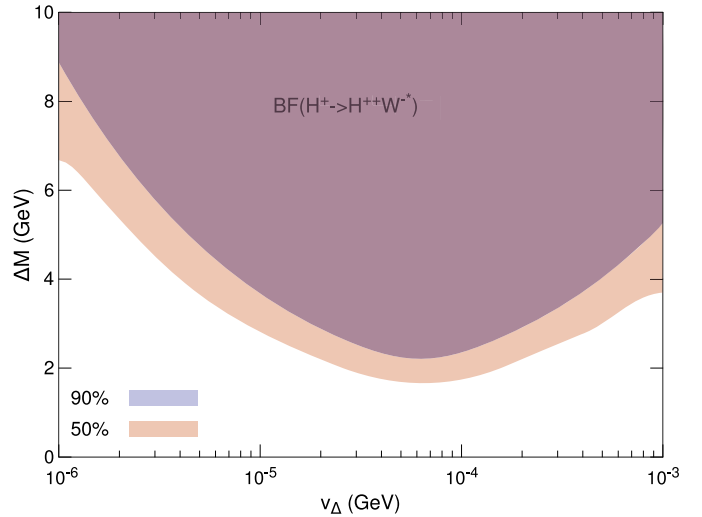

Fig. 2. Branching fraction of $H^{\pm} \to H^{\pm\pm}W^{\mp*}$ in the $v_\Delta - \Delta M$ plane for $M_{H^{++}} = 300$ GeV. The purple and pink regions denote the parameter space where BF($H^{\pm} \to H^{\pm\pm}W^{\mp*}$) is greater than 90% and 50% respectively. (For interpretation of the references to color in this figure, the reader is referred to the web version of this article.)

pair-production of doubly-charged bosons and thus may result in a more stringent constraints on doubly-charged boson mass $M_{H^{++}}$.

One of our aims in this Letter is to revise the constraints on $M_{H^{++}}$ obtained by CMS and ATLAS after including all the processes which contribute to pair-production of doubly-charged bosons. We use CTEQ6L [16] parton distribution function (PDF) and the renormalization/factorization scale is set at $2M_{H^+}$. CALCHEP [17] is used to generate the parton level events for the relevant processes. Then, using LHEF [18] interface, we pass these parton level events to PYTHIA [19] for fragmentation and initial/final state radiations. We use PYCELL, a toy calorimeter in PYTHIA, for hadronic level simulation for finding jets using a cone algorithm. For a more realistic simulation, we utilize the same analysis strategy as employed by CMS and ATLAS Collaborations [3,4] in the study of doubly-charged boson. We use selection criteria for four-lepton events from Table 3 of the CMS paper [3]. As for the same-sign dilepton analysis which was performed by ATLAS, we put following selection criteria. Leptons must have a transverse momentum above 20 GeV and be well isolated. In pairs where the higher-p_T lepton is an electron, it is required to have $p_T > 25$ GeV. All pairs of electrons or muons with the same electric charge are considered. The invariant mass of the lepton pair must be larger than 15 GeV, and for $e^\pm e^\pm$ the region close to the Z-boson mass (70 GeV $< m(e^\pm e^\pm) <$ 110 GeV) is excluded due to a large background from $Z \to e^+e^-$ events with an electron charge misidentification.

In Fig. 3, we plot exclusion region in the $M_{++} - \Delta M$ plane obtained by including all the processes contributing to $H^{++}-H^{--}$ pair-production for NH and IH in Eq. (12). In the left panel, we utilize the four-lepton analysis as performed by CMS and in the right panel, the same-sign dilepton analysis of ATLAS has been utilized to constrain the parameter space in the $M_{++} - \Delta M$ plane. Our results, depending on the neutrino mass patterns (NH or IH), go significantly beyond the analysis of Fig. 2 in Ref. [10] which used preliminary data obtained by the CMS in 2011. For our analysis, we consider three values of triplet vacuum expectation value, namely, $v_\Delta = 10^{-6}$ GeV, 5×10^{-5} GeV and 2×10^{-4} GeV. We find that the parameter space is the most constrained for $v_\Delta = 5 \times 10^{-5}$ GeV and the least for $v_\Delta = 2 \times 10^{-4}$ GeV. Notice that the constraints are weaker for NH as BF($H^{++} \to e^+e^+ + \mu^+\mu^+ + e^+\mu^+$) is con-
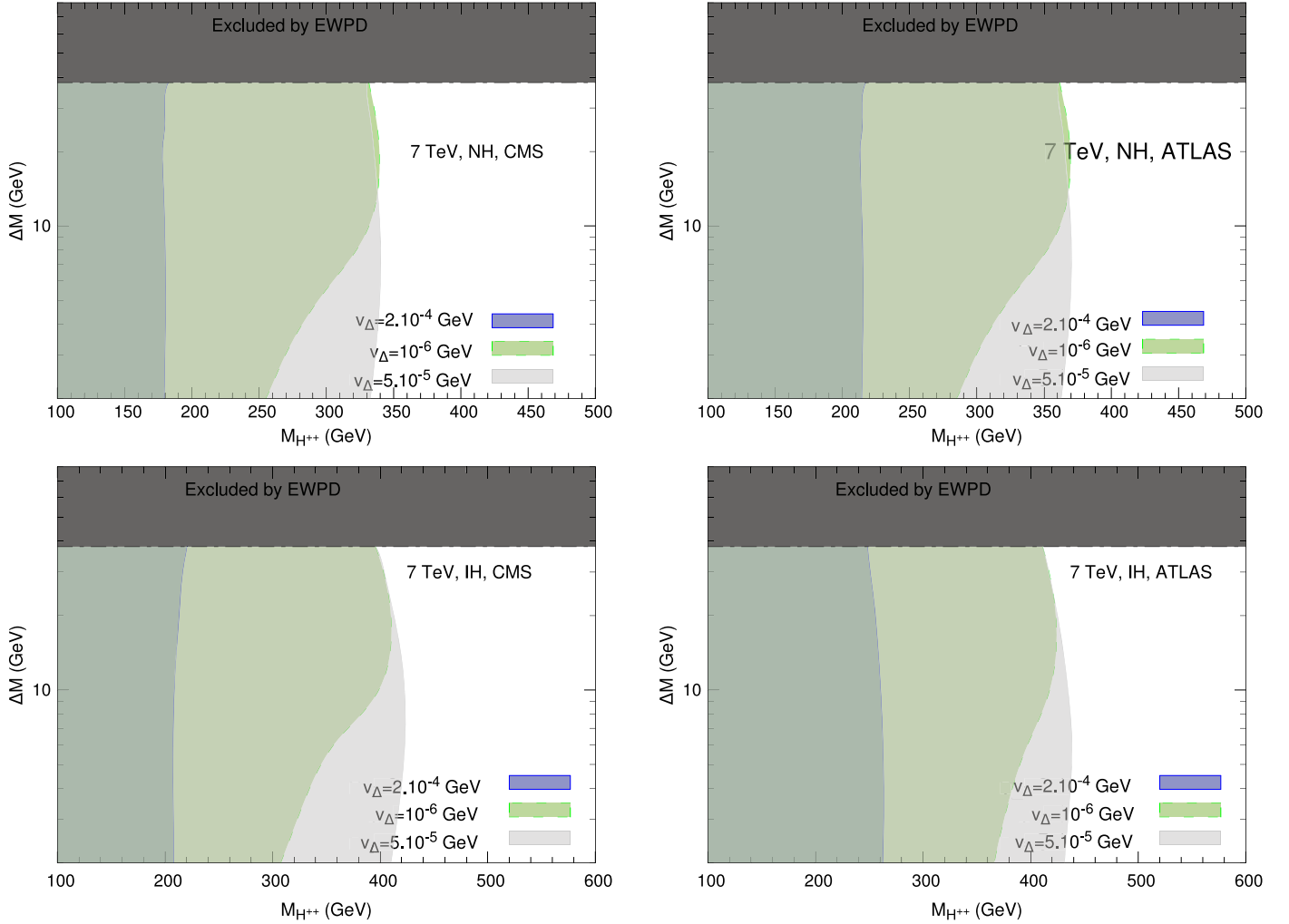
Fig. 3. Exclusion region in the $M_{H^{++}}$–ΔM plane utilizing CMS (left) and ATLAS (right) analyses for $v_\Delta = 2 \times 10^{-4}$ GeV, 10^{-6} GeV and 5×10^{-5} GeV. For the upper (lower) panels, the NH (IH) neutrino mass pattern is assumed.

siderably smaller than that for the case of IH as can be seen from the table (12).

From Fig. 1, one finds that BF($H^{\pm\pm} \to \ell^\pm \ell^\pm$) is around 15%–40% for $v_\Delta = 2 \times 10^{-4}$ GeV when $M_{H^{++}}$ is 200–500 GeV while for $v_\Delta = 5 \times 10^{-5}$ GeV and smaller, it is over 80%. Thus, the constraints on the doubly-charged boson mass gets stronger for smaller v_Δ. Note that in Fig. 3 there appears a peculiar behavior for $v_\Delta = 10^{-6}$ GeV. When mass splitting ΔM is very small, the bound on charged Higgs mass is very loose while for relatively large $\Delta M > 10$ GeV, constraints become comparable to the case of $v_\Delta = 5 \times 10^{-5}$ GeV. This behavior has to do with the branching fraction of, e.g., $H^+ \to H^{++} W^+$ shown in Fig. 2. One can see that BF($H^\pm \to H^{\pm\pm} W^{\mp*}$) is always below 90% for $v_\Delta = 10^{-6}$ GeV unless $\Delta M > 10$ GeV, and thus none of the processes for triplet production mentioned above will contribute to pair-production of H^{++} unless $\Delta M > 10$ GeV. On the other hand, for $v_\Delta = 5 \times 10^{-5}$ GeV, the BF is more than 90% even for ΔM as low as 2 GeV and thus have large number of events for H^{++}–H^{--} production which lead to stringent constraints on $M_{H^{++}}$ even for small ΔM.

The gray region in $M_{H^{++}}$–ΔM plane for $\Delta M > 38$ GeV is excluded by considering electroweak precision constraints on λ_5, hence on ΔM [12]. This bound on ΔM is found to be independent of doubly-charged boson mass $M_{H^{++}}$. One can also see that bounds obtained by utilizing ATLAS analysis are stronger than

those obtained by following CMS. This is because ATLAS Collaboration have considered same-sign di-lepton signals coming from the decay of only one doubly-charged boson in pair-production while CMS have looked at four-lepton final states. It is clear that ATLAS would have large number of signal events as compared to CMS.

4. SS4L signals at LHC8/13

Apart from the well-studied same-sign di-lepton signals, there can appear also a novel phenomenon of same-sign tetra-leptons indicating the neutral triplet–antitriplet oscillation [13]. Such a signal would be an indisputable evidence for the discovery of a doubly-charged boson in type II seesaw. For this to occur, one needs a condition for the oscillation parameter:

$$x \equiv \frac{\delta M_{HA}}{\Gamma_{\Delta^0}} \gtrsim 1 \qquad (15)$$

where δM_{HA} is the mass splitting (14) between two real degrees of freedom of the neutral triplet boson, and $\Gamma_{\Delta^0} \simeq \Gamma(\Delta^0 \to H^+ W^{-*})$. Arising from the lepton number violating effect, δM_{HA} is proportional to ξ^2 and thus can be comparable to the decay rate of $\Gamma_{\Delta^0} \approx G_F^2 \Delta M^5 / \pi^3$ which is also quite suppressed for a small mass gap $\Delta M \approx M_{H^0} - M_{H^+}$. Once the oscillation parameter is determined, one can calculate the production cross-sections for the same-sign tetra-lepton final states from the following formula [13]:
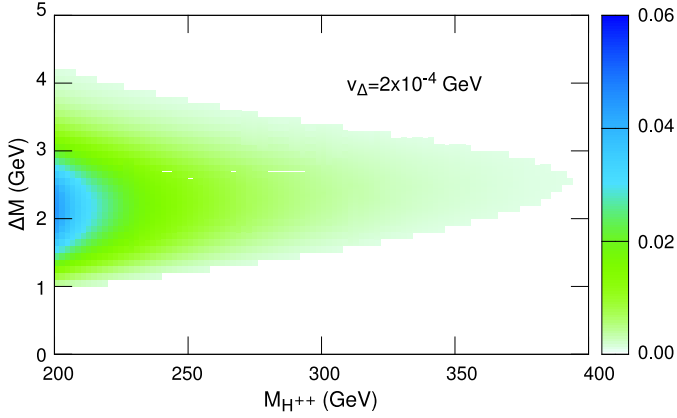
Fig. 4. The quantity χ_B (17) in the $M_{H^{++}}$–ΔM plane for $v_\Delta = 2 \times 10^{-4}$ GeV. (For interpretation of the references to color in this figure legend, the reader is referred to the web version of this article.)

$$\sigma\left(4\ell^\pm + n W^{\mp *}\right)$$

$$= \left\{ \sigma\left(pp \to H^\pm \Delta^{0(\dagger)}\right) \left[\frac{x^2}{2(1+x^2)}\right] \mathrm{BF}\left(\Delta^{0(\dagger)} \to H^\pm W^{\mp *}\right) \right.$$

$$+ \sigma\left(pp \to \Delta^0 \Delta^{0\dagger}\right) \left[\frac{2+x^2}{2(1+x^2)} \frac{x^2}{2(1+x^2)}\right]$$

$$\times \left[\mathrm{BF}\left(\Delta^{0(\dagger)} \to H^\pm W^{\mp *}\right)\right]^2 \right\}$$

$$\times \left[\mathrm{BF}\left(H^\pm \to H^{\pm\pm} W^{\mp *}\right)\right]^2 \left[\mathrm{BF}\left(H^{\pm\pm} \to \ell_i^\pm \ell_j^\pm\right)\right]^2. \quad (16)$$

To analyze the effect of oscillation, let us define,

$$\chi_B \equiv \left[\frac{x^2}{2(1+x^2)}\right] \mathrm{BF}\left(\Delta^{0(\dagger)} \to H^\pm W^{\mp *}\right) \left[\mathrm{BF}\left(H^\pm \to H^{\pm\pm} W^{\mp *}\right)\right]^2$$

$$\times \left[\mathrm{BF}\left(H^{\pm\pm} \to \ell_i^\pm \ell_j^\pm\right)\right]^2, \quad (17)$$

which determines the viability of SS4L signal originating from process $pp \to H^+ \Delta^{0\dagger}$ at the LHC. It includes factors such as $\mathrm{BF}(\Delta^{0(\dagger)} \to H^\pm W^{\mp *})$, $\mathrm{BF}(H^\pm \to H^{\pm\pm} W^{\mp *})$ and oscillation probability which are indispensable components for the occurrence of SS4L signal at the LHC.

In Fig. 4, we plot χ_B in the plane of $M_{H^{++}}$–ΔM. One can see that χ_B is sizable only in the limited range of $\Delta M = (1, 4)$ GeV at $M_{H^{++}} = 200$ GeV. The blue region in the figure is the area where probability of SS4L signal is maximum. Lower values of ΔM are disfavored because $\mathrm{BF}(\Delta^{0(\dagger)} \to H^\pm W^{\mp *})$ and $\mathrm{BF}(H^\pm \to H^{\pm\pm} W^{\mp *})$ are too suppressed (as seen from Fig. 2) while higher values are suppressed due to increase in Γ_{Δ^0} which leads to very small oscillation probability ($x^2 \ll 1$). For larger $M_{H^{++}}$, Γ_{Δ^0} also increases and thus leads to narrowing down of allowed parameter space in the $M_{H^{++}}$–ΔM plane.

Let us now discuss if observable same-sign tetra-lepton signals can be obtained in the allowed parameter region of Fig. 3. For this analysis, we consider two values of $v_\Delta = 5 \times 10^{-5}$ GeV and 2×10^{-4} GeV for which $M_{H^{++}}$ larger than about 400 and 200 GeV is allowed respectively, and discard $v_\Delta = 10^{-6}$ GeV which gives a vanishingly small oscillation probability χ_B. We consider all triplet production processes which can contribute to SS4L signal at 8 TeV (LHC8) and 13 TeV (LHC13) of LHC with 20 fb^{-1} and 100 fb^{-1} of integrated luminosities respectively.

In Fig. 5, we plot the number of SS4L events achievable for $v_\Delta = 2 \times 10^{-4}$ GeV at LHC8 with 20 fb^{-1} of the integrated luminosity assuming the IH neutrino mass structure. The signal numbers are smaller for NH. The number of events for $v_\Delta =$
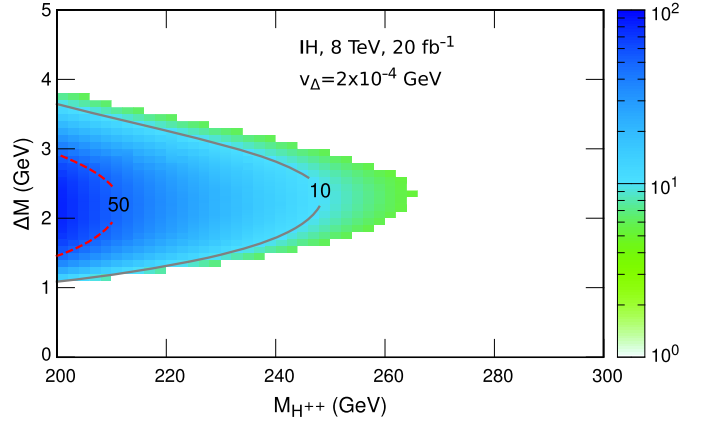
Fig. 5. Contour plots for SS4L signal numbers in the $M_{H^{++}}$–ΔM plane at LHC8 for $v_\Delta = 2 \times 10^{-4}$ GeV. Here the IH neutrino mass structure is taken.

5×10^{-5} GeV at LHC8 are very low for $M_{H^{++}} > 400$ GeV, and thus this case is not interesting. We find that a sizable number of SS4L events can be obtained in the range of $\Delta M \sim (1, 4)$ GeV for which the oscillation probability is large enough. In order to see SS4L events at LHC8, we need $M_{H^{++}} \lesssim 260$ GeV which, however, is almost ruled out by the current ATLAS results shown in the lower left panel of Fig. 3.

Fig. 6 shows the number of SS4L events at LHC13 with 100 fb^{-1} of the integrated luminosity for $v_\Delta = 2 \times 10^{-4}$ GeV (left) and $v_\Delta = 5 \times 10^{-5}$ GeV (right) taking NH (upper) and IH (lower) for the neutrino mass structure. As expected from the table (12), more leptonic final states are obtained for IH and thus better sensitivities for SS4L events are obtained. If we assume that 10 SS4L events would be sufficient for the claim of H^{++} discovery, then for $v_\Delta = 2 \times 10^{-4}$ GeV, H^{++} can be probed up to 330 GeV at LHC13 in the case of IH. On the other hand, for $v_\Delta = 5 \times 10^{-5}$ GeV, H^{++} can be probed up to 750 GeV at LHC13. In the case of NH with $v_\Delta = 2 \times 10^{-4}$ GeV, observable signals can be obtained only for $M_{H^{++}} < 200$ GeV which is excluded by the current ATLAS data, whereas $M_{H^{++}}$ up to 550 GeV can lead to observable SS4L signals for $v_\Delta = 5 \times 10^{-5}$ GeV.

5. Conclusion

Type II seesaw model of neutrino mass generation introduces an $SU(2)_L$ triplet boson which contains a doubly-charged scalar and thereby leads to peculiar collider signatures. Collider phenomenology of the triplet boson sector depends on three parameters: the mass gap $\Delta M = M_{H^\pm} - M_{H^{\pm\pm}} \approx M_{H^0/A^0} - M_{H^+}$ among the triplet components $H^{\pm\pm}$, $H^\pm$ and H^0/A^0, the doubly-charged boson mass $M_{H^{\pm\pm}}$, and the triplet vacuum expectation value v_Δ (or the leptonic Yukawa coupling f_{ij} of the triplet). Considering the case of $\Delta M > 0$ for which the doubly-charged boson is the lightest, we studied the LHC bounds on its mass depending on ΔM and v_Δ utilizing the current CMS and ATLAS search for the doubly-charged boson from same-sign di-lepton (SS2L) resonances. In the range of $\Delta M \gtrsim 1$ GeV, the gauge decays of the heavier triplet components end up with producing doubly-charged bosons and associated W^*'s and thus augment the search limit of $M_{H^{\pm\pm}}$. On the other hand, the bound is weakened for larger v_Δ for which the leptonic decay modes of the triplet bosons are more suppressed. The results are summarized in Fig. 3 taking three representative values of v_Δ for the cases of two neutrino mass hierarchies (NH and IH).

When the tiny mass splitting between two neutral components H^0 and A^0 is comparable to the decay rate Γ_{H^0/A^0}, there can appear an oscillation phenomenon which leads to pair-production of
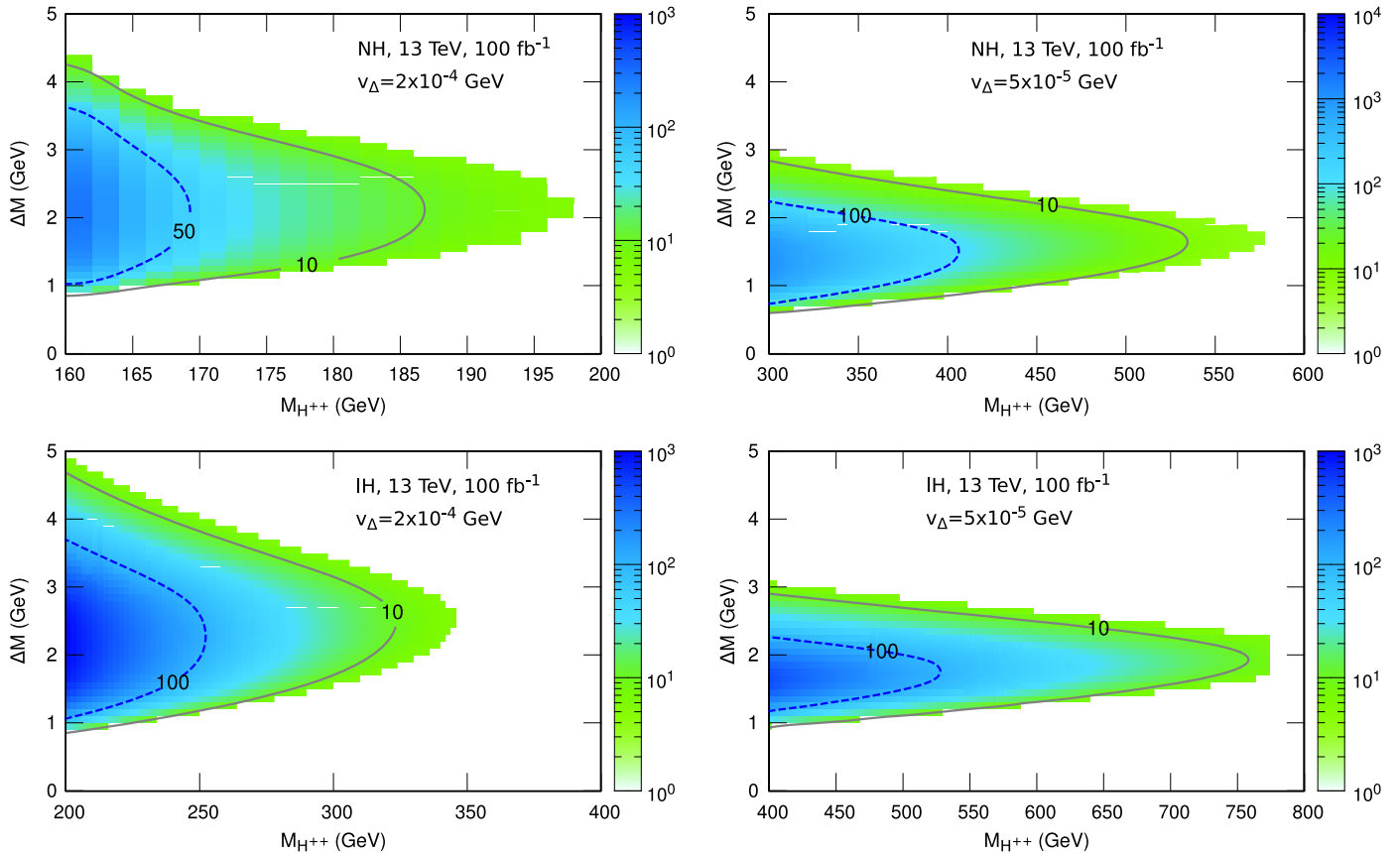
Fig. 6. Contour plots for SS4L signal numbers in the $M_{H^{++}} - \Delta M$ plane at LHC13 for $v_\Delta = 2 \times 10^{-4}$ GeV and 5×10^{-5} GeV. The upper (lower) panels assume NH (IH) for the neutrino mass pattern.

same-sign doubly-charged bosons and thus same-sign tetra-lepton (SS4L) final states at the LHC. For allowed parameter region from the current SS2L search, we analyzed the prospects for observing SS4L signals at LHC8 and LHC13 which are summarized in Figs. 5 and 6. Note that more leptonic final states (with e and μ) are produced in the case of IH compared to NH and thus better search sensitivity is obtained for IH. Observable SS4L signature can be obtained only in the limited region of $\Delta M \sim 1$–4 GeV and probed up to $M_{H^{\pm\pm}} \sim 750$ GeV at the LHC13 with 100 fb^{-1} of the integrated luminosity for the most probable case of IH with $v_\Delta = 5 \times 10^{-5}$ GeV. On the other hand, the SS4L search becomes much more restricted due to the reduced number of leptonic final states or smaller oscillation probability for larger or smaller v_Δ. In the case of $v_\Delta = 2 \times 10^{-4}$ GeV, SS4L signals can be observable up to $M_{H^{\pm\pm}} \sim 350$ GeV.

Acknowledgements

References

[1] M. Magg, C. Wetterich, Phys. Lett. B 94 (1980) 61;
T.P. Cheng, L.F. Li, Phys. Rev. D 22 (1980) 2860;
J. Schechter, J.W.F. Valle, Phys. Rev. D 22 (1980) 2227;
G. Lazarides, Q. Shafi, C. Wetterich, Nucl. Phys. B 181 (1981) 287;
R.N. Mohapatra, G. Senjanovic, Phys. Rev. D 23 (1981) 165.
[2] E.J. Chun, K.Y. Lee, S.C. Park, Phys. Lett. B 566 (2003) 142, arXiv:hep-ph/0304069.
[3] S. Chatrchyan, et al., CMS Collaboration, Eur. Phys. J. C 72 (2012) 2189, arXiv:1207.2666 [hep-ex].
[4] G. Aad, et al., ATLAS Collaboration, Eur. Phys. J. C 72 (2012) 2244, arXiv:1210.5070 [hep-ex].
[5] A.G. Akeroyd, M. Aoki, Phys. Rev. D 72 (2005) 035011, arXiv:hep-ph/0506176.
[6] P. Fileviez Perez, T. Han, G.-y. Huang, T. Li, K. Wang, Phys. Rev. D 78 (2008) 015018, arXiv:0805.3536 [hep-ph].
[7] A.G. Akeroyd, C.-W. Chiang, N. Gaur, J. High Energy Phys. 1011 (2010) 005, arXiv:1009.2780 [hep-ph].
[8] K. Huitu, J. Maalampi, A. Pietila, M. Raidal, Nucl. Phys. B 487 (1997) 27, arXiv:hep-ph/9606311.
[9] A.G. Akeroyd, H. Sugiyama, Phys. Rev. D 84 (2011) 035010, arXiv:1105.2209 [hep-ph].
[10] A. Melfo, M. Nemevsek, F. Nesti, G. Senjanovic, Y. Zhang, Phys. Rev. D 85 (2012) 055018, arXiv:1108.4416 [hep-ph].
[11] M. Aoki, S. Kanemura, K. Yagyu, Phys. Rev. D 85 (2012) 055007, arXiv:1110.4625 [hep-ph].
[12] E.J. Chun, H.M. Lee, P. Sharma, J. High Energy Phys. 1211 (2012) 106, arXiv:1209.1303 [hep-ph];
E.J. Chun, H.M. Lee, P. Sharma, arXiv:1305.0329 [hep-ph].
[13] E.J. Chun, P. Sharma, J. High Energy Phys. 1208 (2012) 162, arXiv:1206.6278 [hep-ph];
E.J. Chun, P. Sharma, arXiv:1304.5059 [hep-ph];
E.J. Chun, P. Sharma, Phys. Lett. B 722 (2013) 86, arXiv:1301.1437 [hep-ph].
[14] T. Han, B. Mukhopadhyaya, Z. Si, K. Wang, Phys. Rev. D 76 (2007) 075013, arXiv:0706.0441 [hep-ph].
[15] S. Kanemura, K. Yagyu, H. Yokoya, arXiv:1305.2383 [hep-ph].
[16] J. Pumplin, A. Belyaev, J. Huston, D. Stump, W.K. Tung, J. High Energy Phys. 0602 (2006) 032, arXiv:hep-ph/0512167.
[17] A. Pukhov, arXiv:hep-ph/0412191.
[18] J. Alwall, A. Ballestrero, P. Bartalini, S. Belov, E. Boos, A. Buckley, J.M. Butterworth, L. Dudko, et al., Comput. Phys. Commun. 176 (2007) 300, arXiv:hep-ph/0609017.
[19] T. Sjostrand, S. Mrenna, P.Z. Skands, J. High Energy Phys. 0605 (2006) 026, arXiv:hep-ph/0603175.